Electronic supplementary information

L-Dopa and dopamine conjugated naphthalenediimides modulate amyloid β toxicity

Madhu Ramesh,[a,†] Pandeeswar Makam,[a,†] Chandrashekhar Voshavar,[a,†] Harshavardhan Khare,[b] Kolla Rajasekhar,[a] Suryanarayanarao Ramakumar,[b] Thimmaiah Govindaraju[a*]

[a]Bioorganic Chemistry Laboratory, New Chemistry Unit, Jawaharlal Nehru Centre for Advanced Scientific Research, Jakkur P.O., Bengaluru 560064, Karnataka, India. E-mail: tgraju@jncasr.ac.in.

[b] Department of Physics, Indian Institute of Science, Bengaluru 560012, India.

[†] These authors contributed equally.

Synthesis of amyloid beta (Aβ11-25) peptide. Aβ11-25 (EVHHQKLVFFAEDVG) peptide was synthesized following standard 9-fluorenylmethoxycarbonyl (Fmoc) chemistry on an automated peptide synthesiser (Syro II, MultiSynTech). Rink amide resin (Novabiochem) was used as a solid support in the synthesis. Amino acids were coupled using HBTU as the activating reagent, DIPEA in DMF. For the deprotection of Fmoc 40% piperidine in DMF was used. The peptide was purified using a reverse-phase (RP) preparative HPLC on C18 column at 40 °C. Product purity was greater than 95%, as ascertained by analytical HPLC. The molecular mass of the peptide was verified by HRMS (Q-TOF) (Agilent 6538 UHD HRMS/Q-TOF) analysis.

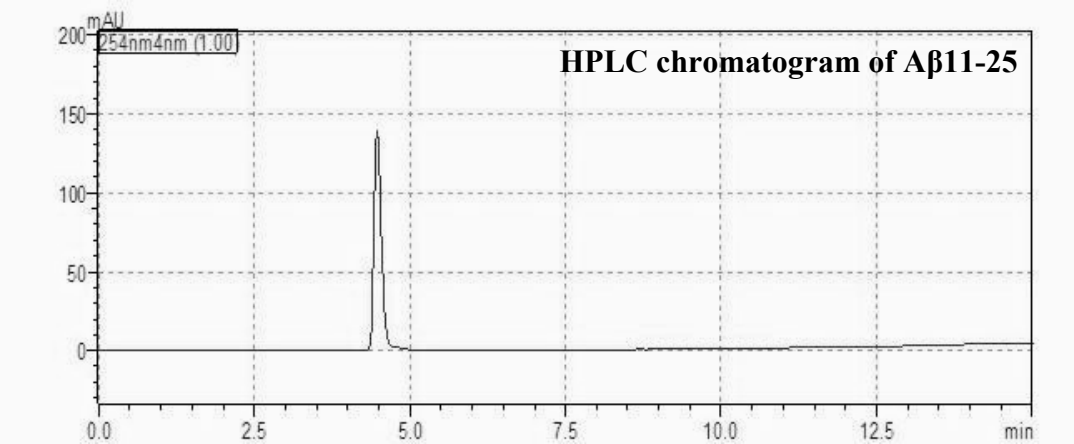

HPLC Conditions:

System: Shimadzu HPLC, **Column:** Phenomenex, RP-C18 (5µm, 4.6 × 250 mm)
Mobile Phase: Water:ACN, 70:30, v/v with 0.1% TFA, **Injection Volume:** 15 µL
Flow Rate: 0.8 mL/min, **Run Time:** 15 min, **Typical Column Pressure:** 65-70 Bar
Detection: PDA detector

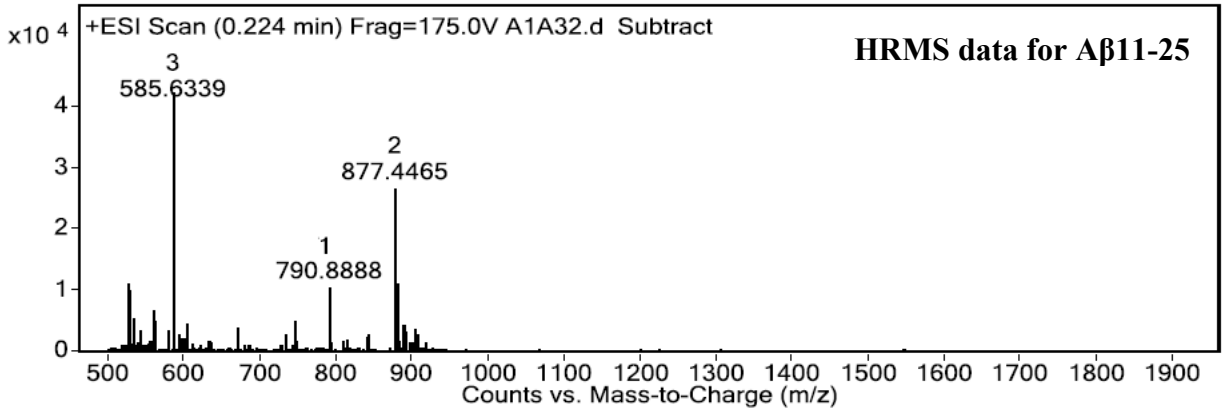

The calculated molecular weight of Aβ11-25 $[(M+2H)/2]^{+2}$= 877.4445 obtained mass = 877.4465

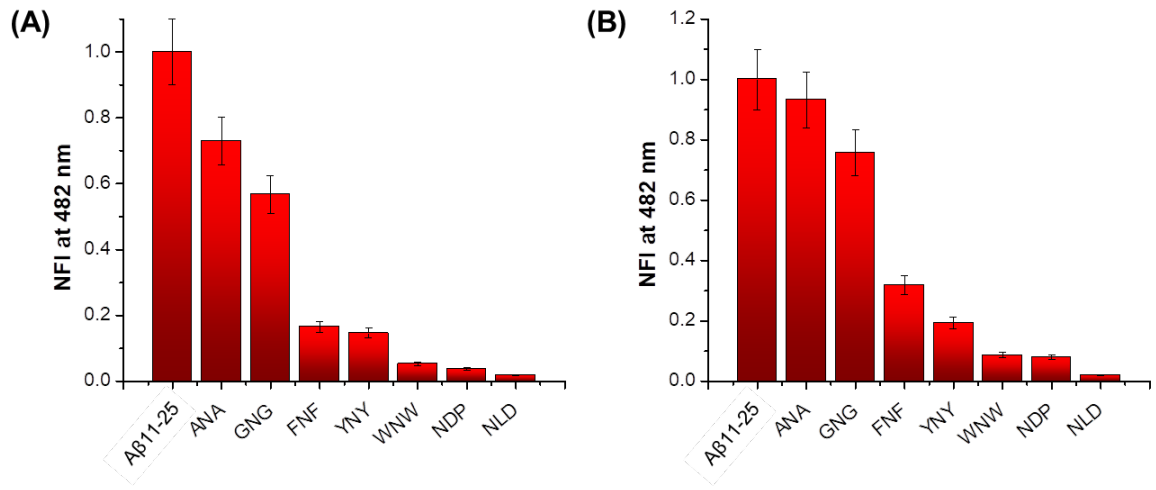

Fig. S1 ThT fluorescence assay. (A) Effects of NDI conjugates on the aggregation of Aβ11-25 (200 μM) after 48 h incubation at 1:1 molar ratios of Aβ11-25:NDI conjugate and the plot of ThT fluorescence intensity at 482 nm as a function of NDI conjugates (**ANA**, **GNG**, **FNF**, **YNY**, **WNW**, **NDP** and **NLD**). (B) Effects of NDI conjugates on the disaggregation of Aβ11-25 (200 μM) pre-formed aggregates (after 48 h incubation) and further incubation for 24 h at 1:1 molar ratios of Aβ11-25: NDI conjugate. The normalized fluorescence intensity (NFI) of ThT at 482 nm in presence of Aβ11-25 (control) and upon treatment with NDI conjugates.

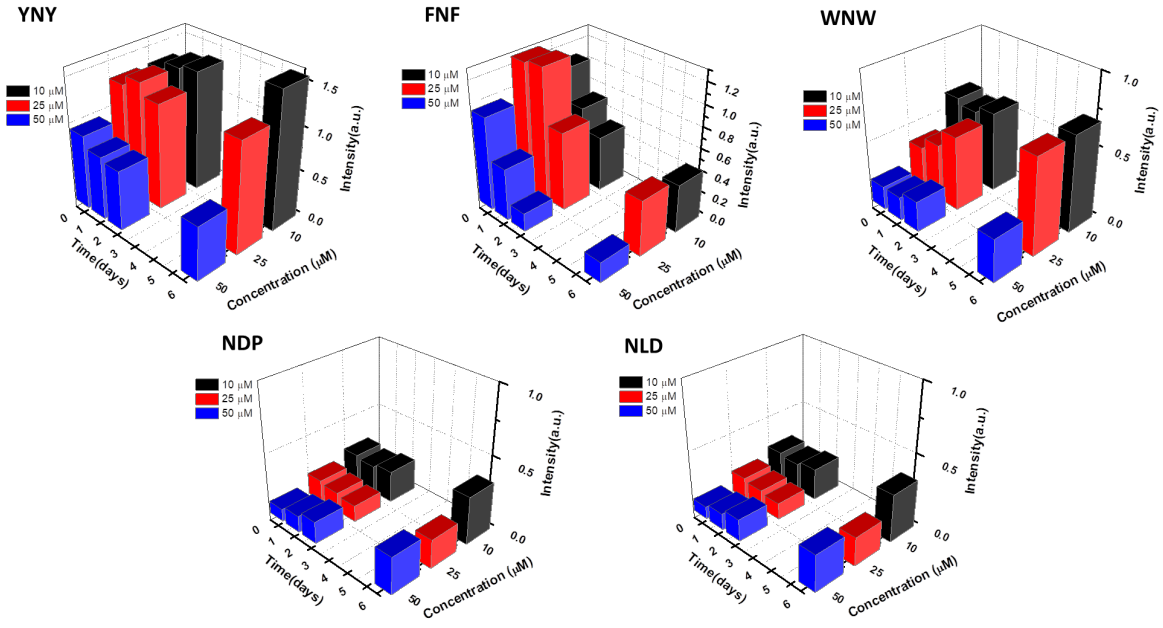

Fig. S2 ThT fluorescence assay for the time and concentration-dependent dissolution of Aβ11-25 aggregates with NDI conjugates (**YNY**, **FNF**, **WNW**, **NDP** and **NLD**).

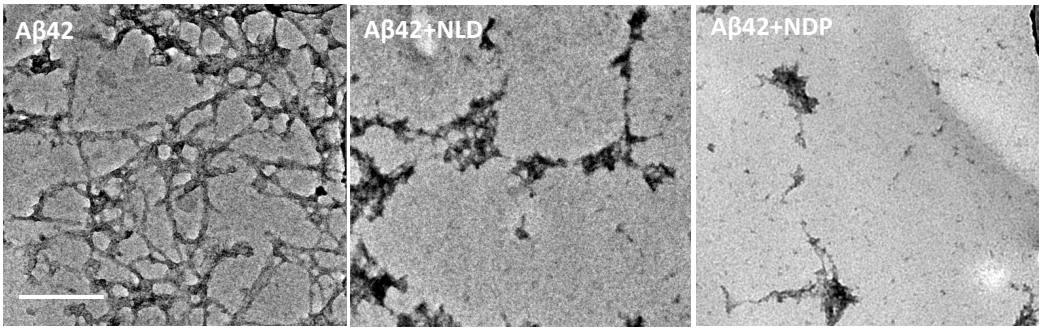

Fig. S3 Transmission electron microscopy (TEM) study to evaluate the effect of NDP and NLD on Aβ42 aggregation. NDP and NLD were incubated with 20 μM of Aβ42 monomer at 37 °C in 1:1 (Aβ42:NDI modulator) stoichiometry for 24 h and the samples were visualised under TEM.

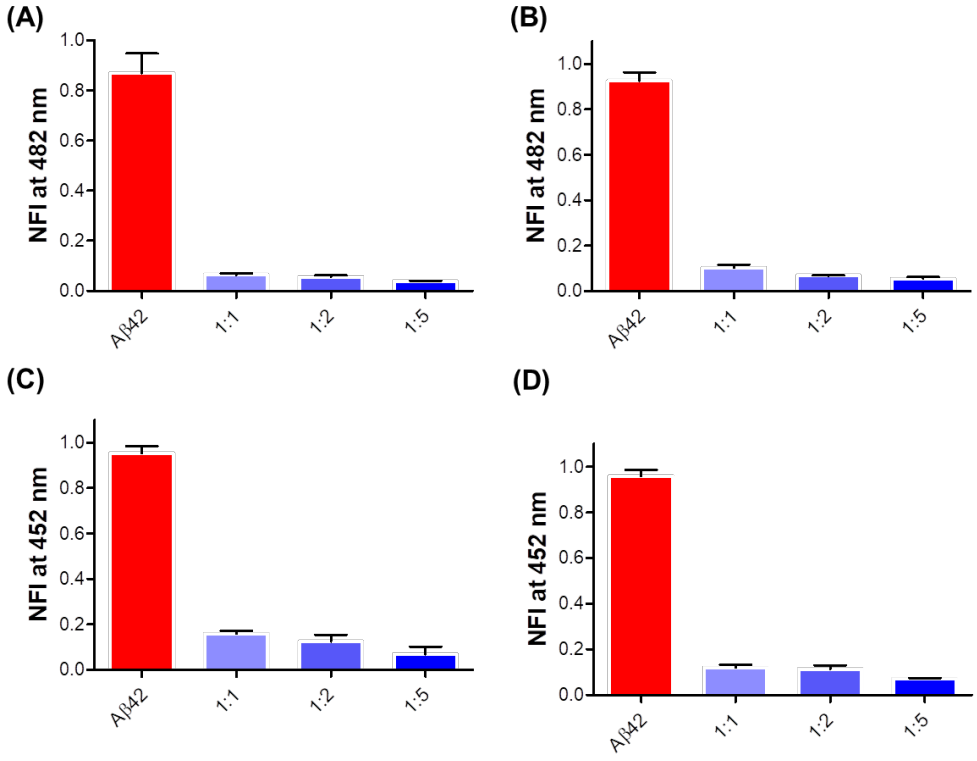

Fig. S4 Inhibition of Aβ42 aggregation (50 μM) with **NDP** (A) and **NLD** (B) by ThT assay. Dissolution of pre-formed Aβ42 aggregates (50 μM) with **NDP** (C) and **NLD** (D) by ThT assay. Values are the normalized fluorescence intensity (NFI) at 482 nm compared to that of the control (Aβ42).

In silico docking protocols

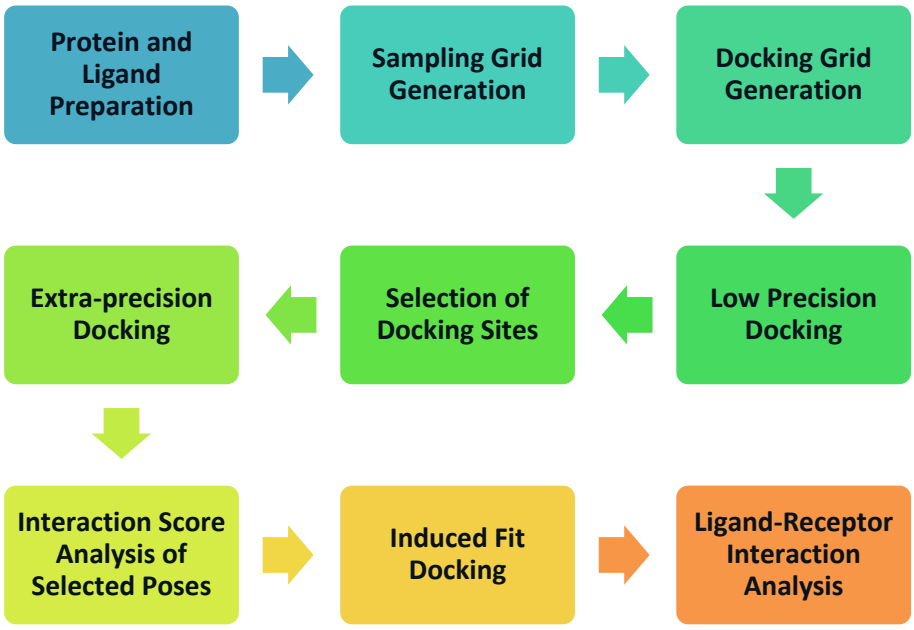

Protocol for blind docking

1. Receptor was prepared by adding missing hydrogen atoms followed by short minimization using OPLS 2005 force field.

2. Python scripts were written to wrap the receptor in a rectangular grid with equispaced points. The spacing between the points should be such that the inner boxes of docking grid do not intersect. (Please refer to the Schrödinger Software documentation for the definitions of inner and outer box used in Glide docking protocol.) In our case, the inner box size was taken as the spacing between the points (5 Å). This rectangular grid can be viewed as a collection of cubic cells of 5 Å sides. The centroids of these cells are considered as sampling points on which the docking grids were generated in the next step. Filtering is performed such that every sampling point has at least one receptor atom in any of the 26 neighbouring cells and at least one of the 26 neighbouring cells is empty. This ensures that the retained sampling points are near the surface of the receptor and not inside the receptor at the same time.

3. Docking grids were generated for all the sampling points.

4. Ligand was prepared for docking.

5. Docking was performed for all the grids in batch mode using xglide script in Schrödinger software suite.

6. Ensemble of multiple poses corresponding to every grid was generated.

Following is the pictorial representation of this protocol.

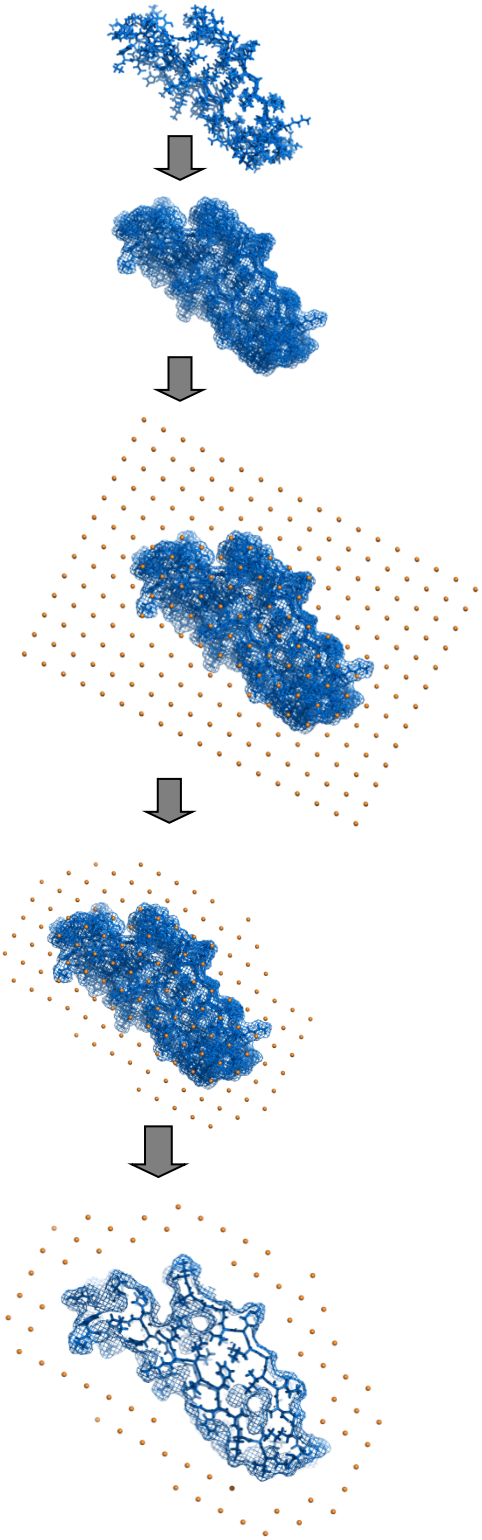

Amyloid β structure stick model (viewing down the fibril axis)

Surface representation of amyloid β structure

Amyloid beta structure is wrapped in a rectangular grid with equispaced sampling points.

Extra sampling points are removed based on the criteria described in the protocol (Refer the protocol given above).

A section of amyloid β structure embedded in the grid showing correct wrapping of the receptor in the sampling grid.

Blind docking results. Multiple docked poses obtained with different scores. (Amyloid beta receptor is shown as yellow sphere model.)

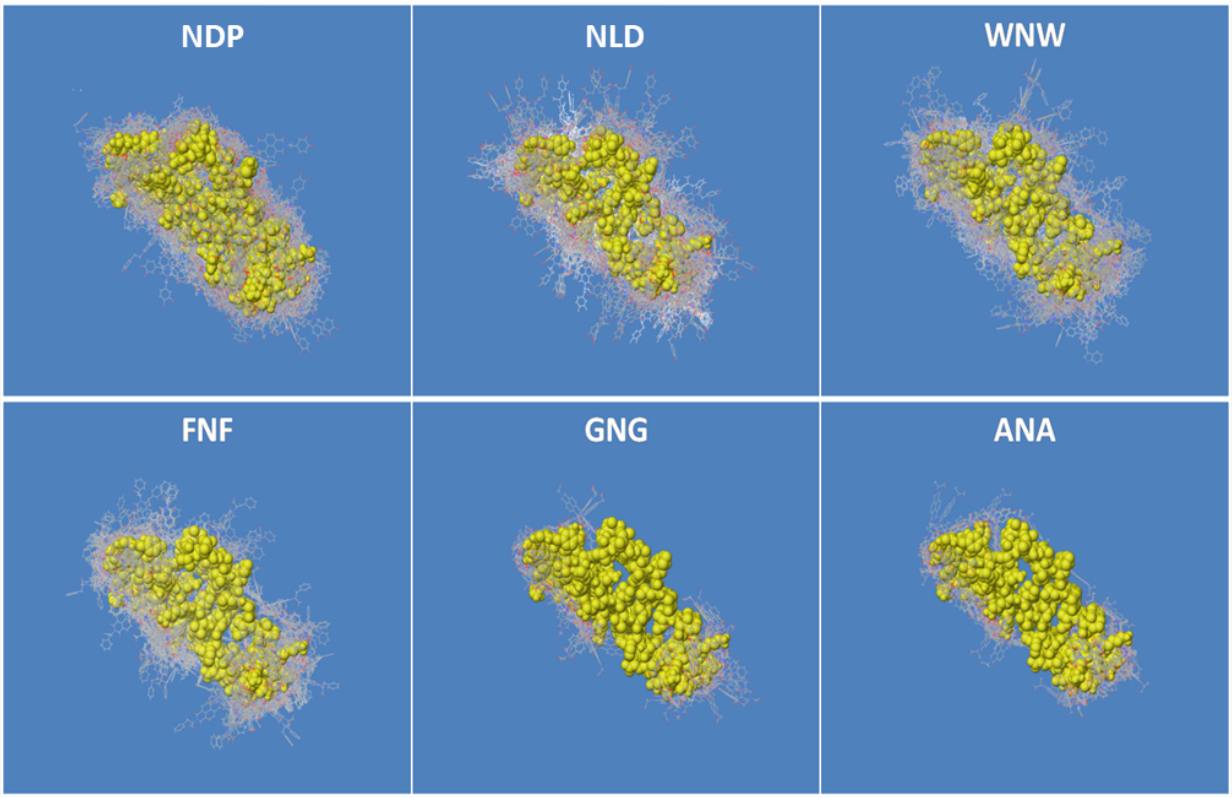

Table S1. XP docking scores for IIGLM region

Inhibitor	XP docking score
NDP	-6.95
NLD	-8.37
WNW	-5.29
FNF	-5.10
GNG	
ANA	

Table S2. XP docking scores for KLVFFA region

Inhibitor	XP docking score
NDP	-3.18
NLD	-6.67
WNW	-5.56
FNF	-5.17
GNG	-4.81
ANA	-4.21

IFD scores. To quantitatively test whether experimental results match with the computational docking results, we have calculated the correlation of the docking scores with the experimental aggregation inhibition. The docking scores and normalized fluorescence intensities of ThT assays of aggregation inhibition were examined for the correlation analysis. Pearson's correlation coefficient and Spearman's rank-order correlation coefficient were calculated. As can be seen in Table S3, the docking scores for the IIGLM region show good correlation with the experimental results of Aβ fibril induced fit docking (IFD) scores. However, the IFD scores for KLVFFA site seem to be poorly correlated with the experimental results. The reason for this is the inconsistent docking score of NDP, which shows poor IFD score for KLVFFA region despite being a good inhibitor of Aβ aggregation in vitro. The correlation coefficients calculated excluding NDP are shown in Table S4. Note the distinct increase in both Pearson's and Spearman's correlation coefficients for KLVFFA after excluding NDP. Overall, the correlation analysis indicates validity of the agreement between computational docking and experimental results.

Table S3 IFD scores for IIGLM and KLVFFA regions

Ligand Name	**Docking score for IIGLM**	**Docking score for KLVFFA**	**Experimental results**
NLD	-365.03	-363.82	0.091
NDP	-362.54	-355	0.086
WNW	-360.4	-359.69	0.359
FNF	-351.7	-360.81	0.553
ANA	0	-356.56	0.897
GNG	0	-355.89	NA
Pearson's correlation with experimental results	**0.83**	**0.25**	
Spearman's rank-order correlation with experimental results	**1.00**	**-0.10**	

Table S4 IFD scores for IIGLM and KLVFFA regions excluding NDP

Ligand Name	Docking score for IIGLM	Docking score for KLVFFA	Experimental results
NLD	-365.03	-363.82	0.091
WNW	-360.4	-359.69	0.359
FNF	-351.7	-360.81	0.553
ANA	0	-356.56	0.897
GNG	0	-355.89	NA
Pearson's correlation with experimental results	**0.85**	**0.92**	
Spearman's rank-order correlation with experimental results	**1.00**	**0.80**	

Docking with 2BEG. PDB ID 2BEG is solid state NMR structure of Aβ1-42. Although being full length construct, the refined residues are only leucine 17 onwards. Moreover the number of refined chains is 5 which is less than other two structures 2LMO and 2LMN. All the ligands were docked with 2BEG to confirm the problems with insufficient number of refined chains and missing lysine at position 16.

Table S5. XP docking scores for PDB ID 2BEG

Inhibitor	IIGLM	KLVFFA
NDP	-3.66	-4.20
NLD	-4.68	-3.92
WNW	-3.47	-2.07
FNF	-1.52	-0.85
GNG	-2.99	
ANA		

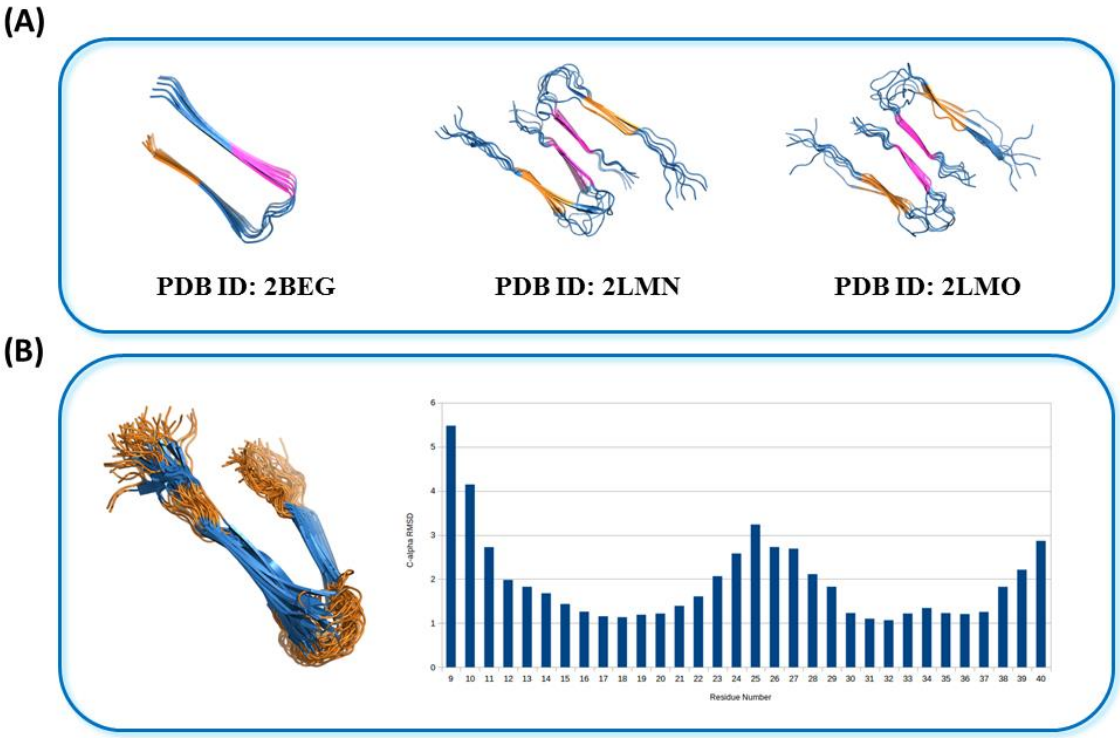

Fig. S5 (A) Aβ42 structures obtained from protein data bank. (B) Residue-wise C-α RMSD for chains A to F of NMR structure 2LMN.

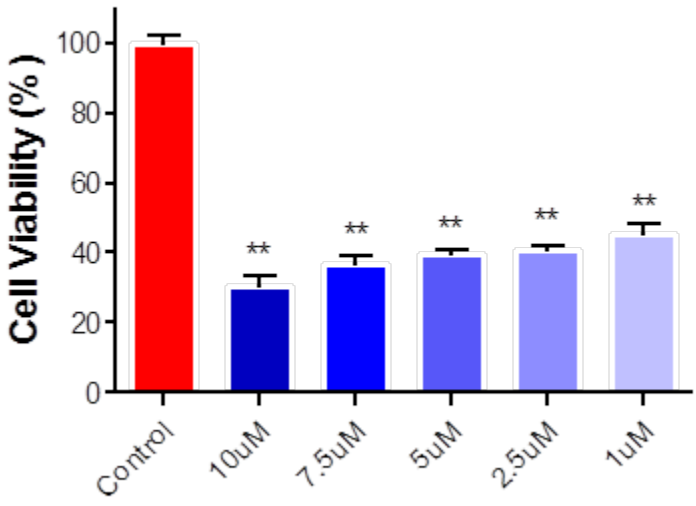

Fig. S6 Concentration-dependent toxicity (1-10 μM) exhibited by Aβ42 aggregates on cell viability of PC12 cells.

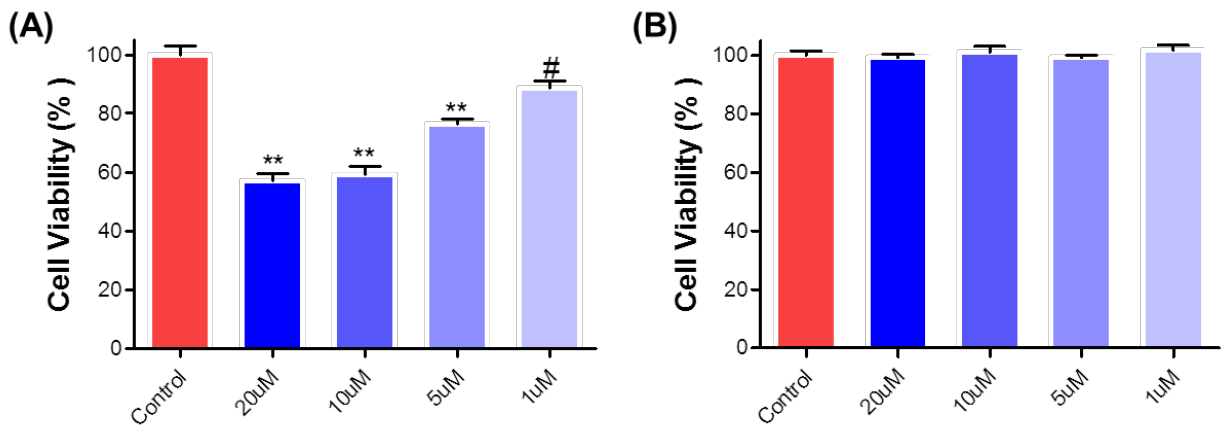

Fig. S7 Effect of NDI modulators on the cell viability of PC12 cells. PC12 cells were incubated with 1, 5, 10 and 20 μM of either **NDP** (A) or **NLD** (B) for 24 h. Values shown are means ± SEM of three independent experiments performed in six to eight replicates. One-way ANOVA analysis followed by Tukey's multiple comparison post hoc test was performed (#$p < 0.05$, **$p < 0.001$ compared to control).

Specific rotations of chiral NDI conjugates

Specific rotation of NDI conjugates at 20 °C in DMSO at concentration of 0.01 gml^{-1} ($[a]_D^{20}$ (c, 0.01, DMSO)

Compound	**ANA**	**WNW**	**YNY**	**FNF**	**NLD**
Specific Rotation $[a]_D^{20}$	-77.7	-363.64	-307.06	-301.34	-318.84

^{1}H and ^{13}C NMR spectra

ANA, FNF and WNW were synthesised and characterised following the reported procedure.[1]

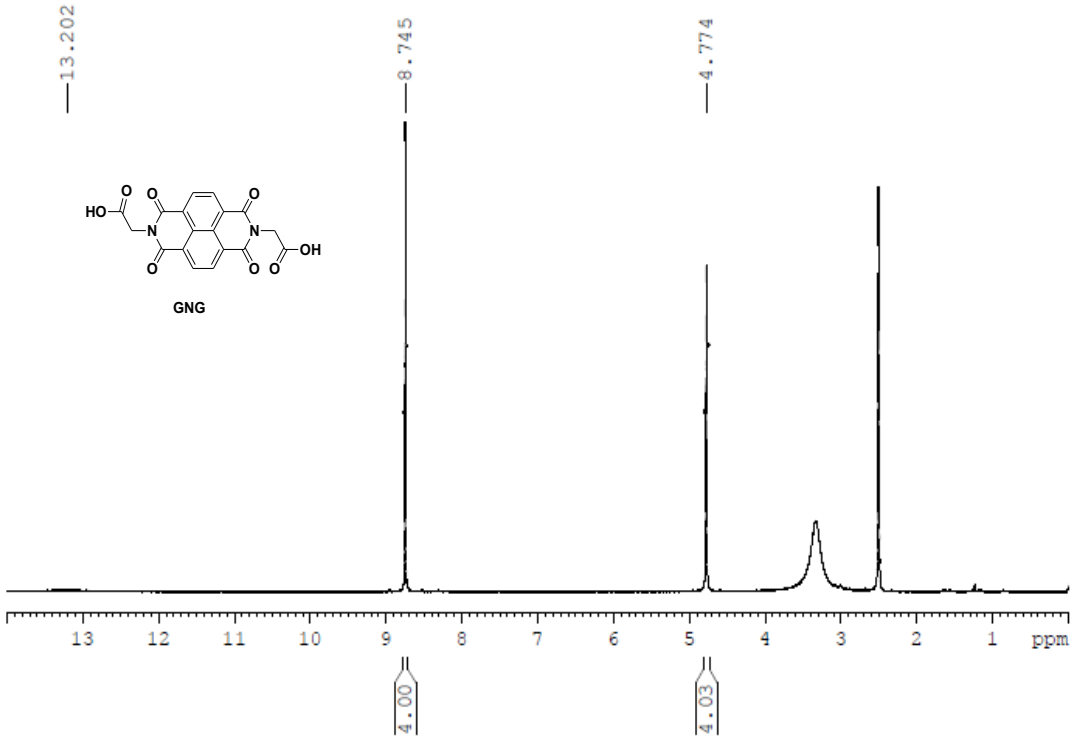

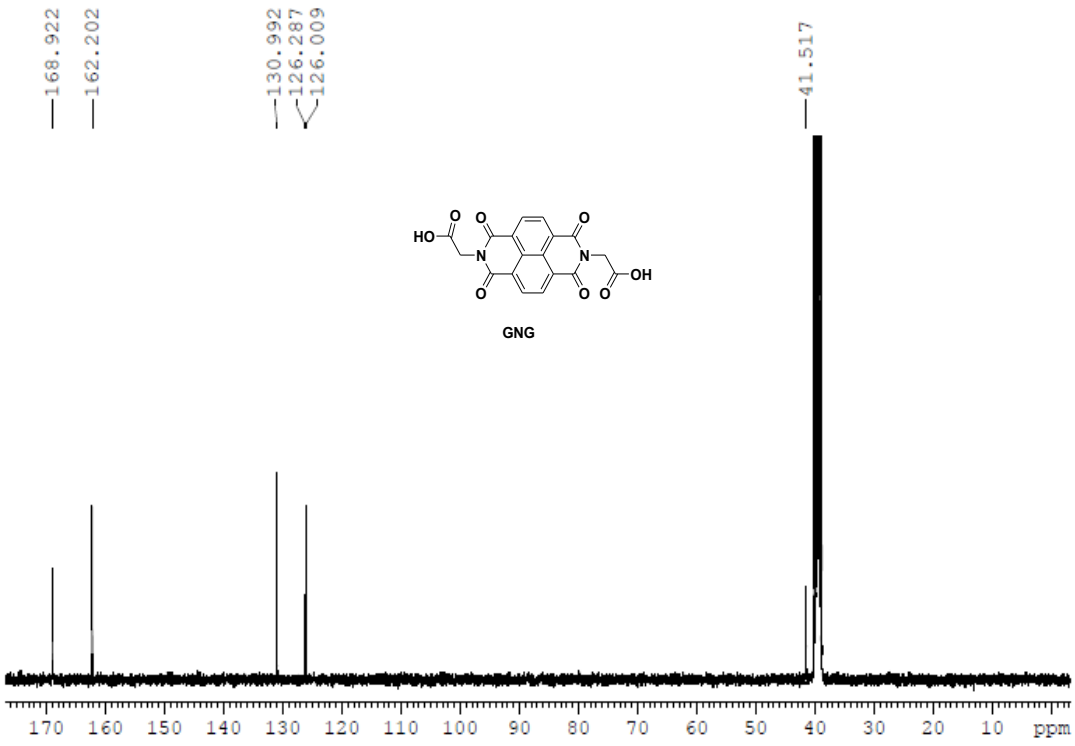

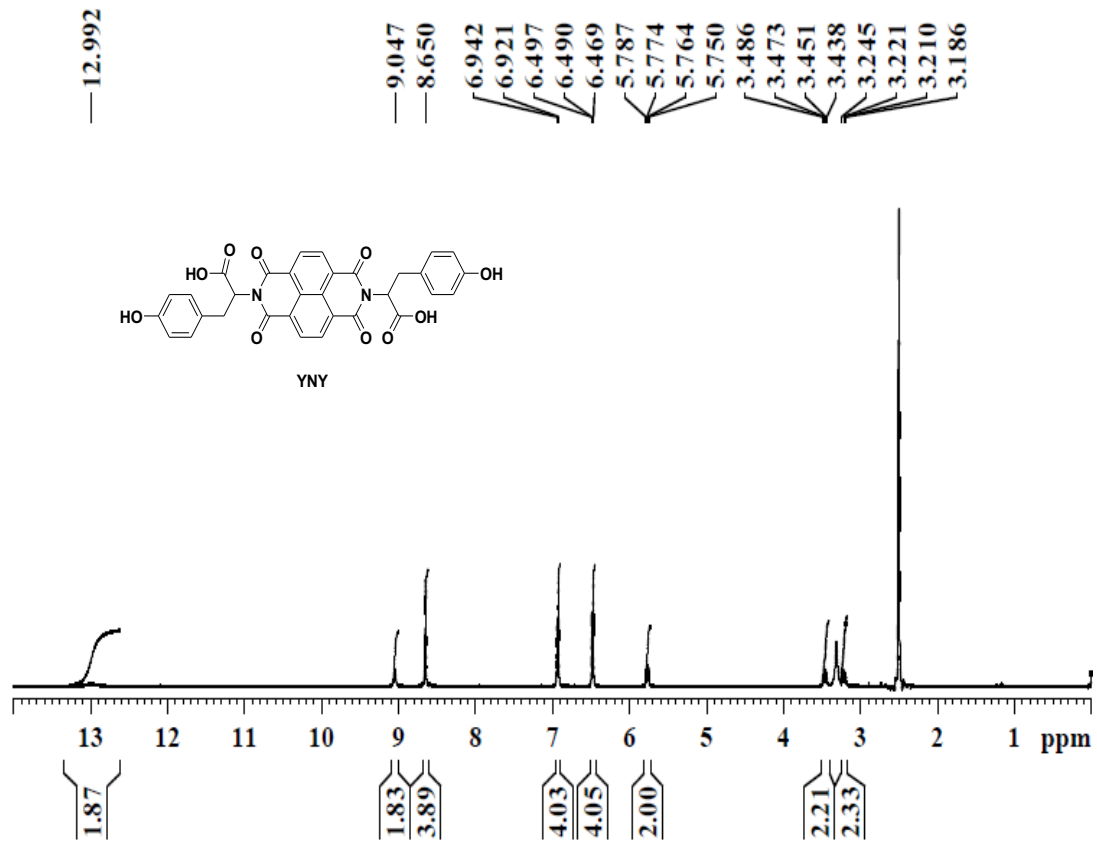
12.992
9.047
8.650
6.942
6.921
6.497
6.490
6.469
5.787
5.774
5.764
5.750
3.486
3.473
3.451
3.438
3.245
3.221
3.210
3.186
YNY
13 12 11 10 9 8 7 6 5 4 3 2 1 ppm
1.87
1.83
3.89
4.03
4.05
2.00
2.21
2.33

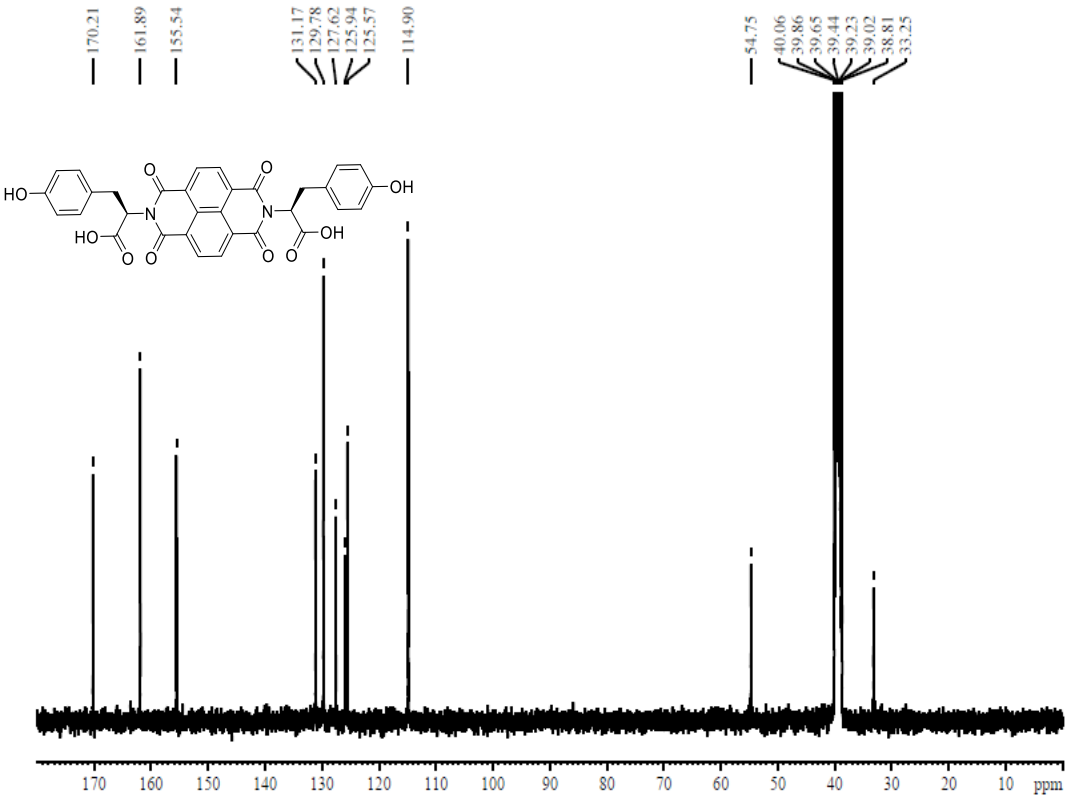
170.21
161.89
155.54
131.17
129.78
127.62
125.94
125.57
114.90
54.75
40.06
39.86
39.65
39.44
39.23
39.02
38.81
33.25
170 160 150 140 130 120 110 100 90 80 70 60 50 40 30 20 10 ppm

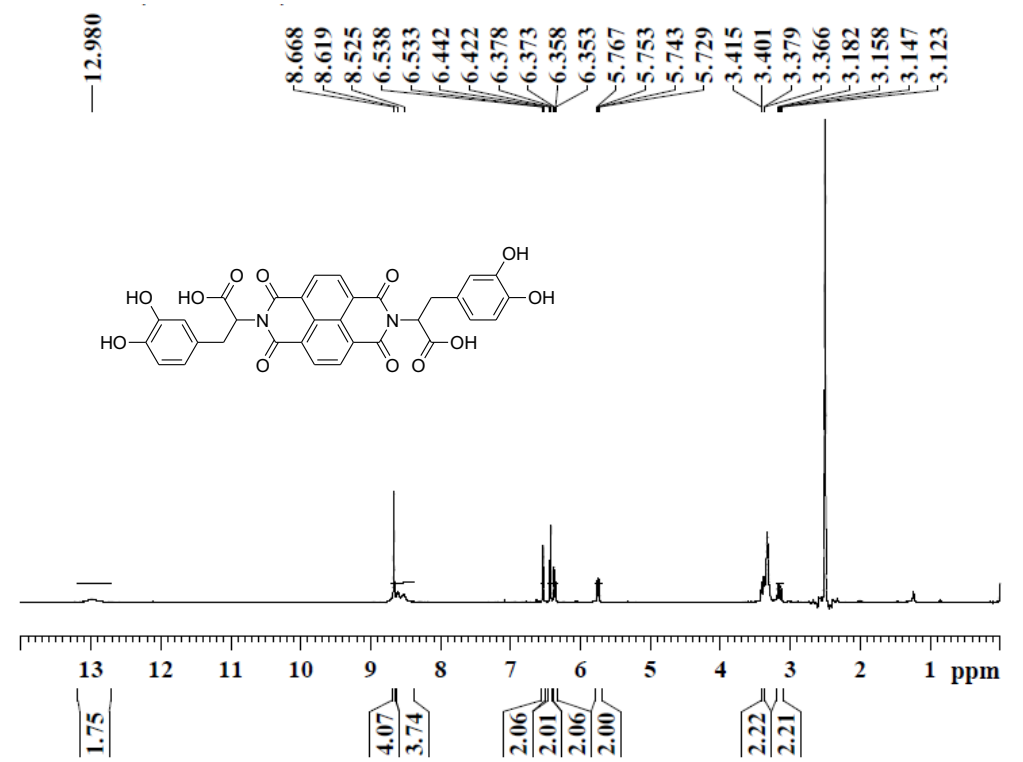
12.980
8.668
8.619
8.525
6.538
6.533
6.442
6.422
6.378
6.373
6.358
6.353
5.767
5.753
5.743
5.729
3.415
3.401
3.379
3.366
3.182
3.158
3.147
3.123
HO
HO
HO
OH
OH
OH
N
N
O
13 12 11 10 9 8 7 6 5 4 3 2 1 ppm
1.75
4.07
3.74
2.06
2.01
2.06
2.00
2.22
2.21

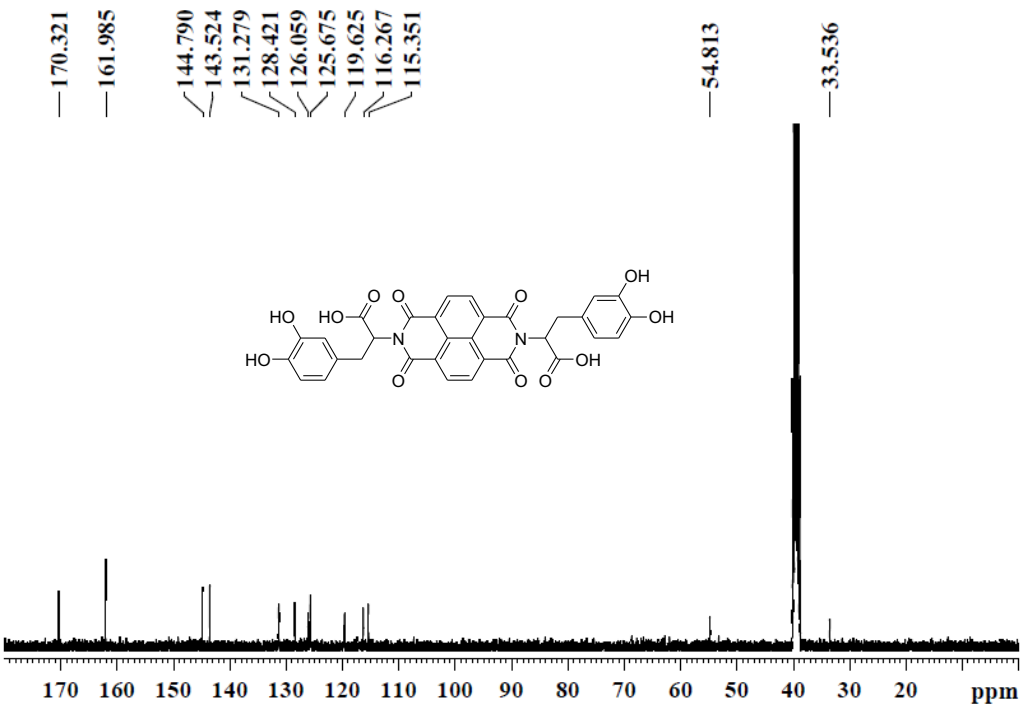
170.321
161.985
144.790
143.524
131.279
128.421
126.059
125.675
119.625
116.267
115.351
54.813
33.536
HO
HO
HO
OH
OH
OH
N
N
O
170 160 150 140 130 120 110 100 90 80 70 60 50 40 30 20 ppm

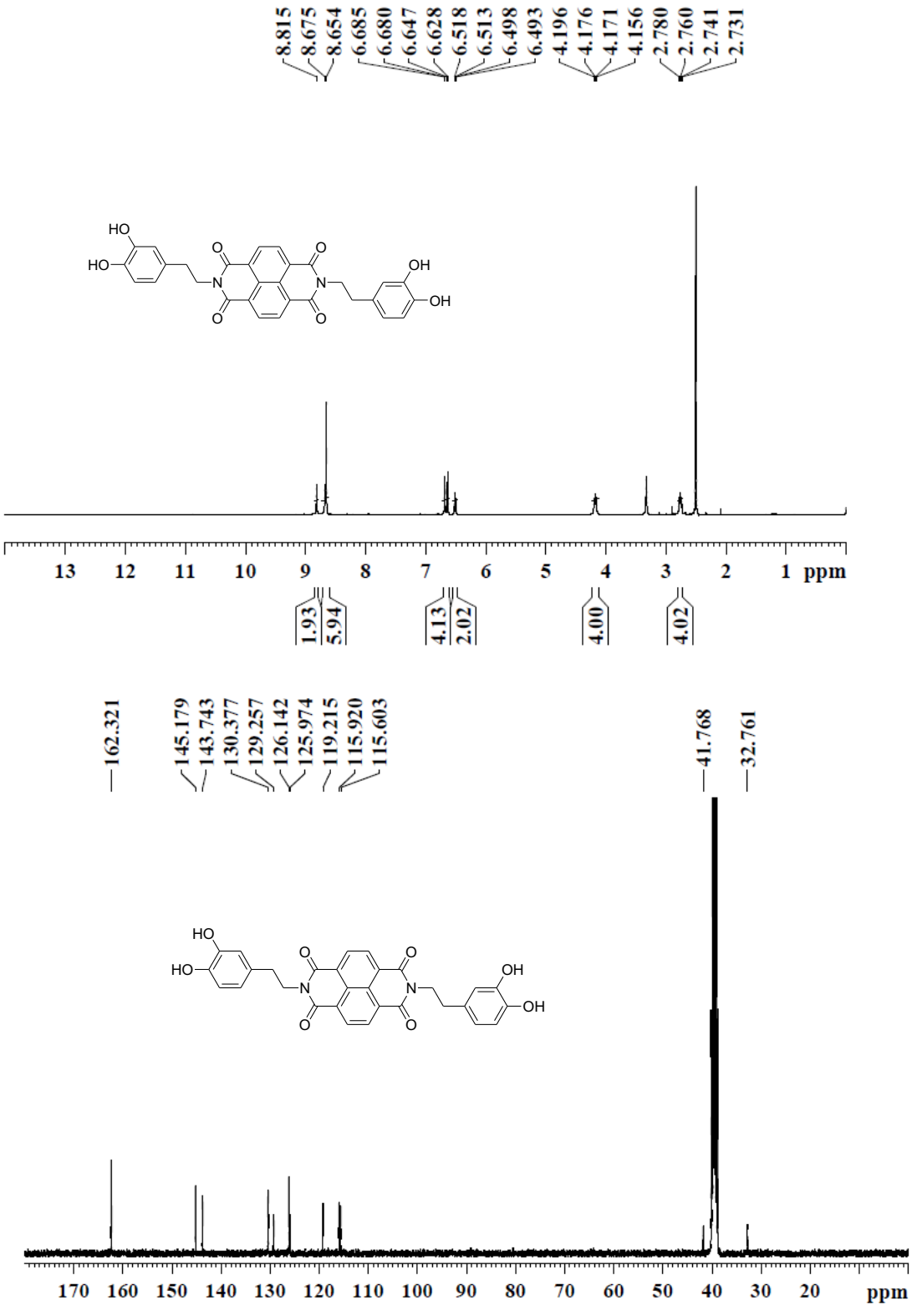
8.815
8.675
8.654
6.685
6.680
6.647
6.628
6.518
6.513
6.498
6.493
4.196
4.176
4.171
4.156
2.780
2.760
2.741
2.731
HO
HO
OH
OH
13 12 11 10 9 8 7 6 5 4 3 2 1 ppm
1.93
5.94
4.13
2.02
4.00
4.02
162.321
145.179
143.743
130.377
129.257
126.142
125.974
119.215
115.920
115.603
41.768
32.761
170 160 150 140 130 120 110 100 90 80 70 60 50 40 30 20 ppm

Reference

1. M. Pandeeswar, H. Khare, S. Ramakumar and T. Govindaraju, *RSC Adv*., 2014, **4**, 20154-20163.